Research Article

Hatem A. Abuelizz, El Hassane Anouar, Nasser S. Al-Shakliah, Mohamed Marzouk, Rashad Al-Salahi*

Structural cytotoxicity relationship of 2-phenoxy(thiomethyl) pyridotriazolopyrimidines: Quantum chemical calculations and statistical analysis

https://doi.org/10.1515/chem-2020-0138
received March 6, 2020; accepted June 3, 2020

Abstract: Previously, a series of pyridotriazolopyrimidines (**1–6**) were synthesized and fully described. The target compounds (**1–6**) were evaluated for their cytotoxicity against MCF-7, HepG2, WRL 68, and A549 (breast adenocarcinoma, hepatocellular carcinoma, embryonic liver, and pulmonary adenocarcinoma, respectively) cell lines using MTT assay. The tested compounds demonstrated cytotoxicity, but no significant activity. To elucidate the structure–cytotoxicity relation of the prepared pyridotriazolopyrimidines, several chemical descriptors were determined, including electronic, steric, and hydrophobic descriptors. These chemical descriptors were calculated in the polarizable continuum model (water as solvent) using density functional theory calculations at B3LYP/6-31+G(d,p). By employing simple linear regression (SLR) and multiple linear regression (MLR) analyses, the impact of the selected descriptors was assessed statistically. The obtained results clearly reveal that the cytotoxicity of pyridotriazolopyrimidines depends on their (i) basic skeleton and (ii) the type of the tested cell. Interestingly, SLR and MLR analyses show that the impact of the selected descriptors is strongly related to the tested cells and basic skeleton of the tested compounds. For instance, the cytotoxicity of subclasses **2a** and **2c–2f** against A459 shows strong correlation with ionization potential, hardness (η), and hydrophobicity ($\log P$) with a correlation coefficient of 99.86% and a standard deviation of 0.53.

Keywords: pyridotriazolopyrimidines, DFT, cytotoxicity, MLR, SLR

1 Introduction

Cancer is a complex ailment and remains a major health concern despite intensive efforts to elucidate its biology and develop more efficacious antitumor agents. Notably, resistance often develops in patients treated with anticancer agents, resulting in disease progression and poor prognosis. Hence, several chemotherapeutic compounds, approved as adjuvant therapy for several types of cancers, have demonstrated inadequate response rates, approximately between 30% and 70%. Furthermore, resistance can occur as a consequence of decreased drug activity even prior to drug exposure (primary) or during/after the treatment course (acquired). The ever-growing resistance to anticancer agents is a leading cause of cancer-related mortality worldwide. Therefore, the discovery of new antitumor agents with minor side effects is a crucial task and a highly pursued aim in contemporary pharmaceutical chemistry [1–5].

Heterocyclic compounds including nucleic acids, novel substances, the plurality of medicine, and synthetic/natural dyes are extensively present in nature. Investigators have attempted to generate diverse heterocyclic structures bearing triazole, quinazoline, benzoquinazoline, pyridine, and pyrimidine moieties presenting numerous biological purposes, which remains an ongoing scientific challenge. The pyridine and pyrimidine platforms are used as precursors in agrochemicals and pharmaceuticals and occur in many bioactive important products such as niacin (antipellagra), isoniazid (antituberculosis), thiamine (vitamin B1), barbiturates (central nervous system depressant),

* **Corresponding author: Rashad Al-Salahi,** Department of Pharmaceutical Chemistry, College of Pharmacy, King Saud University, PO Box 2457, Riyadh 11451, Saudi Arabia, e-mail: ralsalahi@ksu.edu.sa, tel: +966 114 677 194
Hatem A. Abuelizz, Nasser S. Al-Shakliah: Department of Pharmaceutical Chemistry, College of Pharmacy, King Saud University, PO Box 2457, Riyadh 11451, Saudi Arabia
El Hassane Anouar: Department of Chemistry, College of Science and Humanities in Al-Kharj, Prince Sattam bin Abdulaziz University, Al-kharj 11942, Saudi Arabia
Mohamed Marzouk: Chemistry of Natural Products Group, Center of Excellence for Advanced Sciences, National Research Centre, 33 El-Bohouth St. (Former El-Tahrir St.), Dokki 12622, Giza, Egypt

zidovudine (antiretroviral medication), and antiviral and anticancer medications. In contrast, 1,2,4-triazoles are associated with various pharmacological activities, and a large number of predominant triazole drugs have been successfully developed and prevalently used in the treatment of various microbial infections such as fluconazole, posaconazole, and itraconazole (antifungal). Combining these three structure features in one molecule (pyridotriazolopyrimidine) has showed significant pharmacological efficiency as fungicidal, herbicidal, antidiabetic, and antioxidant agents [6–11].

Quantum chemical methods are considered efficient tools to determine molecular electronic properties of intermediate systems, correlating them with their biological activities. Several methods have been applied to explain the relation between the cytotoxicity of active compounds and their chemical descriptors [12–14]. For instance, a PM5 semi-empirical method was reported by Ishihara et al., who proved that the correlation is relatively good for tropolone compounds with a basic skeleton of similar dipole moment (μ), hydrophobicity ($\log P$), hardness (η), electrophilicity (ω), and electronegativity (χ) [15]. Furthermore, the cell line type and the parent skeleton of the evaluated compounds (natural or synthesized) play a crucial role in the cytotoxicity profile. Density functional theory (DFT) methods along with statistical analyses is employed to rationalize and confirm the relationship between the cytotoxicity and their correlated structures. Further studies on 4-hydroxycoumarin and ganoderic acid compounds have been reported by Stanchev et al. and Yang et al., revealing that cytotoxicity correlated with $\log P$, μ, volume (V), and the molecular orbital energies (E_{HOMO} and E_{LUMO}) [16,17] for 4-hydroxycoumarin compounds; HOMO energy, χ, electronic energy, $\log P$, and molecular area (A) are dependable variables to distinguish between higher and lower active ganoderic acid compounds [15].

The cytotoxicity of the targets (**1–6**) was evaluated against four cancer cell lines, namely A549, HepG2, and MCF7 carcinoma cells and WRL 68 cells. Herein, we report the structure–cytotoxicity relationship of 2-phenoxy(thiomethyl)pyridotriazolopyrimidines (**1–6**). We employed the polarizable continuum model (PCM) at the B3LYP/6-31+G(d,p) level of theory to calculate the electronic and steric molecular descriptors of the target pyridotriazolopyrimidines and utilized simple linear regression (SLR) and multiple linear regression (MLR) analyses to determine the correlation between the cytotoxicity of pyridotriazolopyrimidines and the calculated descriptors.

2 Materials and methods

2.1 Cell culture and cytotoxicity assay

The cell lines, HepG2, A549, MCF-7, and WRL 68, were obtained from the American Type Culture Collection (ATCC; Rockville, MD, USA). The cells were cultured in two types of media: minimum essential medium and Roswell Park Memorial Institute 1640 medium, supplemented with 10% fetal bovine serum and 1% (v/v) L-glutamine. The cells were incubated in a CO_2 incubator at 37°C, in a humidified atmosphere containing 5% CO_2 and were subcultured once a week using trypsin/ethylenediaminetetraacetic acid (0.25%/0.02%, v/v) for cell detachment from the flasks. Cells at 60–80% confluency were later used for a 3-(4,5-dimethylthiazol-2-yl)-2,5-diphenyltetrazolium bromide (MTT) assay.

A cell viability test was conducted using the MTT assay [18]. Briefly, 2×10^4 cells/well were seeded in a 96-well plate and incubated with 5% CO_2. After 12 h, the cells were treated with 200 µg/mL for 24 h. Next, 20 µL of the MTT solution was added to each well and incubated for another 4 h. The medium was discarded, and the crystalline deposits in the cells were dissolved in 100 µL of dimethyl sulfoxide. The absorbance of the colored formazan crystals was measured at 520 nm using a microplate reader (Tecan, Austria), and the results were presented as mean values ± standard deviation (SD; $n = 3$).

2.2 DFT calculations

By employing the exchange–correlation hybrid functional B3LYP combined with 6-31+G(d,p) double-ζ Pople-type basis, the geometry optimization and frequency calculations of pyridotriazolopyrimidine derivatives were performed, with polarized and diffuse functions taken into consideration [19]. The absence of imaginary frequencies confirms that the optimized structures are true minima. The choice of B3LYP was based on previous studies [20–22]. The solvent effects were taken into account implicitly by using the PCM, in which, the solute is embedded into a cavity surrounded by solvent described by its dielectric constant [23].

The chemical descriptors selected to correlate with cytotoxicity were as follows: (i) electronic descriptors: frontier molecular orbital energies (E_{HOMO} and E_{LUMO}, which are well accepted as molecular descriptors in medicinal chemistry as they are linked to the capacity of

a molecule to form a charge-transfer complex with its biological receptor), hardness (η), electrophilicity index (ω), electronic affinity (EA), softness (S), ionization potential (IP), electronegativity (χ), dipole moment (μ), and molecular polarizability (α); (ii) steric descriptors: surface area of the molecule (A), volume (V), and its molecular weight (M); and (iii) hydrophobicity descriptor: $\log P$, where P denotes the octanol–water partition coefficient. The calculations of $\log P$ were performed using the Hyperchem Molecular package by means of the atomic parameters derived by Ghose, Pritchett, and Crippen and later extended by Ghose and co-workers. The other descriptors may be obtained at the DFT level of theory [24] by considering: (i) orbital consideration, which is based on Koopman's theorem where IP = $-E_{HOMO}$ and EA = $-E_{LUMO}$ [25]; (ii) energy consideration, which is based on the use of the classical finite difference approximation, IP = $E_{+1} - E_0$ and EA = $E_0 - E_{-1}$ where E_0, E_{-1}, and E_{+1} are the electronic energies of neutral molecule, when adding and removing an electron to the neutral molecule, respectively [24]; and (iii) internally resolved hardness tensor approach [26–28]. Previously, we have reported the structure cytotoxicity activity relationship of 2-thiophen-naphtho (benzo)oxazinone derivatives [29] and compounds isolated from *Curcuma zedoaria* [22] by considering orbital and energy methods in calculating electronic and molecular properties, and the results displayed that both methods give similar results. In another study, De Luca et al. tested the three methods to evaluate the solvent effects on the hardness values of a series of neutral and charged molecules, and they concluded that three methods give similar results in the presence of solvent [30]. Herein, to minimize computational cost of theoretical calculations, we have used the first approach in calculating other chemical descriptors. The Gaussian 16 package was used to perform all DFT calculations [31].

2.3 Statistical analyses

SLR and MLR analyses were performed to determine the regression equations, correlation coefficients R^2, adjusted R^2, and SDs between the calculated descriptors and cytotoxicity of the target compounds. The regression curves and statistical parameters are obtained using the DataLab package (http://www.lohninger.com/datalab/en_home.html).

Ethical approval: The conducted research is not related to either human or animal use.

3 Results and discussion

3.1 Cytotoxicity evaluation

The synthetic methodology for target pyridotriazolopyrimidines (Table 1 and Scheme 1) has been previously described [10,11]. As illustrated in Table 2, the *in vitro* cytotoxicity of pyridotriazolopyrimidines was evaluated against A549, HepG2, MCF-7, and WRL 68 cells using the MTT assay. The percentages of cell viability at 200 µg/mL are presented in Table 2 as the cytotoxicity parameter of the tested pyridotriazolopyrimidines. A considerable cytotoxicity was demonstrated by compounds **1a**, **1b**, **2a**, **2c**, **2e**, **2d**, **2f**, **2i**, **2m**, **4**, **5a**, **5b**, and **6c** against A549

Table 1: The synthesized pyridotriazolopyrimidines (**1–6**)

CPs	R	X	R_1	CPs	X	R	R_1
1a	Oph	O	H	**2k**	O	SCH_3	3-Methylbenzyl
1b	SCH_3	O	H	**2l**	O	SCH_3	4-Chlorobenzyl
2a	Oph	O	Benzyl	**2m**	O	SCH_3	Propyl isoindole
2b	Oph	O	Ethyl	**3a**	S	Oph	H
2c	Oph	O	*p*-NO_2-benzyl	**3b**	S	SCH_3	H
2d	Oph	O	Piperidinoethyl	**4**	—	SCH_3	*S*-Ethyl
2e	Oph	O	Morpholinoethyl	**5a**	—	Oph	Cl
2f	Oph	O	Propyl isoindole	**5b**	—	SCH_3	Cl
2g	SCH_3	O	Ethyl	**6a**	—	Oph	*p*-Methyl aniline
2h	SCH_3	O	Allyl	**6b**	—	Oph	*p*-Ethoxy-aniline
2i	SCH_3	O	Benzyl	**6c**	—	Oph	Isoniazid
2j	SCH_3	O	2-Methylbenzyl	**6d**	—	Oph	NH-OH

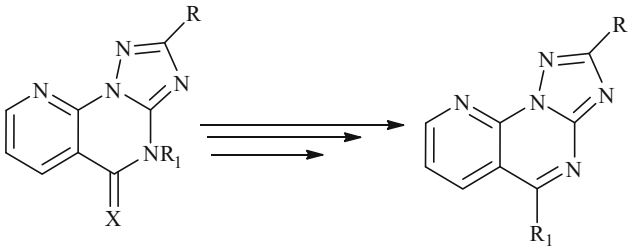

Scheme 1: The synthetic route of the target pyridotriazolopyrimidines (**1–6**).

cells (inhibition% of 33.44–55.87), whereas the significant cytotoxicity against MCF-7 cells (30.75–56.70%) was reported by **2c**, **2f**, **2m**, **4**, and **5b**. In comparison to the aforementioned results, compounds (**2b**, **2d**, **2h**, **2j**, **2k**) and (**2b**, **2h**, **3a**, **5a**) demonstrated moderate effects against A549 and HepG2, respectively. In contrast, **1a**–**b**, **2a**, **3a**, and **6b–d** exhibited moderate effects against MCF-7 cells. The other target compounds failed to demonstrate a significant activity against A549, HepG2, and MCF-7 cell lines. In regard to WRL 68 cells, only **2m** appeared to demonstrate a remarkable activity (19.34%), although **1a**, **1b**, **2e**, **2g**, **2k,** and **5b** showed viability percentages between 10.23 and 12.94%. Based on the findings presented in Table 2, the type of substituent attached to the 2, 4, and 5 positions of the pyridotriazolopyrimidine skeleton can be considered a major determinant for the cytotoxic properties. In the case of the target **2m**, the cytotoxicity increased in the order of MCF-7 > A549 > HepG2 > WRL 68, with **2m** emerging as the most active compound in this series. This could be attributed to the conformation of the heteroalkyl (propyl isoindole) and thiomethyl groups, which might have played a pivotal role in the cytotoxicity profile. The aliphatic C-chain in **2b**, the aromatic(hetero) group in **2c** and **2f**, along with the chloro group in **5a** and **5b** could be responsible factors for their slightly improved cytotoxicity profile against A549, Hep-G2, and MCF-7 cells compared to that of their parents **1a** and **1b**.

3.2 Structure–property relationships

3.2.1 SLR analysis

For the synthesized compounds, SLR analysis was performed to investigate the strength of each descriptor

Table 2: Maximal percentage of cell viability at 200 µg/mL of samples against A549, HepG2, MCF-7, and WRL68 cell lines

CPs	Maximal inhibition (%)			
	A549	HepG2	MCF7	WRL68
1a	42.64 ± 2.18	46.12 ± 16.45	26.75 ± 0.50	11.15 ± 2.75
1b	49.72 ± 8.28	36.22 ± 1.92	24.44 ± 0.66	10.48 ± 0.52
2a	39.19 ± 4.37	39.76 ± 8.46	25.98 ± 2.30	4.50 ± 2.12
2b	25.00 ± 3.28	22.71 ± 2.25	3.94 ± 0.55	5.44 ± 1.71
2c	40.61 ± 8.85	38.15 ± 8.64	38.01 ± 0.64	6.26 ± 1.83
2d	24.03 ± 3.10	34.61 ± 10.56	16.92 ± 1.07	5.87 ± 1.91
2e	34.27 ± 3.13	35.83 ± 3.37	12.61 ± 3.36	12.94 ± 0.78
2f	41.13 ± 3.70	43.76 ± 5.51	35.71 ± 3.58	8.11 ± 2.20
2g	16.50 ± 2.23	10.45 ± 11.66	7.59 ± 9.37	10.78 ± 1.40
2h	27.60 ± 1.96	27.60 ± 1.96	2.11 ± 1.67	5.67 ± 1.89
2i	33.60 ± 2.83	12.72 ± 2.02	1.27 ± 0.67	5.07 ± 3.78
2j	26.96 ± 4.46	16.77 ± 5.76	2.92 ± 2.04	8.62 ± 0.25
2k	26.53 ± 1.39	9.80 ± 3.16	1.43 ± 5.28	10.23 ± 4.62
2l	19.56 ± 4.96	17.66 ± 9.27	5.99 ± 2.20	7.92 ± 0.60
2m	55.87 ± 1.41	40.75 ± 13.12	56.70 ± 0.43	19.34 ± 1.53
3a	23.78 ± 1.76	30.26 ± 5.40	23.94 ± 0.38	1.07 ± 0.89
3b	15.50 ± 6.66	15.50 ± 6.66	4.83 ± 2.35	6.65 ± 2.20
4	41.05 ± 1.98	13.73 ± 0.75	30.75 ± 0.66	8.40 ± 0.36
5a	33.44 ± 1.73	29.31 ± 4.94	10.50 ± 0.58	6.70 ± 1.29
5b	39.71 ± 1.07	14.69 ± 1.61	35.34 ± 1.02	11.05 ± 2.47
6a	20.54 ± 2.51	13.51 ± 7.53	14.15 ± 0.81	3.39 ± 1.43
6b	7.33 ± 11.74	5.94 ± 7.79	21.92 ± 1.25	5.73 ± 1.29
6c	34.53 ± 1.91	47.37 ± 7.76	20.15 ± 5.26	3.58 ± 3.44
6d	3.79 ± 8.89	3.72 ± 15.13	25.95 ± 2.93	7.12 ± 2.15

Table 3: Maximal percentage of cell viability at 200 µg/mL of samples against A549, HepG2, MCF-7, and WRL68 cell lines and molecular descriptors calculated at B3LYP/6-31+G(d,p) of the synthesized compounds

CPs	IP	EA	χ	η	ω	α	μ	A	V	log P	M	Maximal inhibitions			
												A459	HepG2	MCF-7	WRL76
1a	6.42	2.31	4.37	4.11	2.32	287.43	2.51	321.98	346.56	2.73	279.08	42.64	46.12	26.75	11.15
1b	6.38	2.30	4.34	4.08	2.31	230.63	2.32	266.82	281.63	1.03	233.04	49.72	36.22	24.44	10.48
2a	6.61	2.24	4.43	4.37	2.24	314.88	2.92	367.65	399.76	2.96	307.11	39.19	39.76	25.98	4.50
2c	6.68	3.13	4.91	3.55	3.40	421.72	6.54	465.27	514.86	4.42	414.11	40.61	38.15	38.01	6.26
2d	6.18	2.26	4.22	3.92	2.27	403.76	2.99	474.87	524.07	3.32	390.18	24.03	34.61	16.92	5.87
2e	6.36	2.27	4.31	4.10	2.27	392.61	2.70	464.35	511.75	2.26	392.16	34.27	35.83	12.61	12.94
2f	6.64	2.67	4.66	3.97	2.73	474.49	5.48	534.19	591.29	3.49	466.14	41.13	43.76	35.71	8.11
2g	6.32	2.23	4.27	4.10	2.23	263.17	2.95	310.79	333.02	1.62	261.07	16.50	10.45	7.59	10.78
2h	6.34	2.24	4.29	4.10	2.25	280.63	2.80	328.23	351.03	2.01	273.07	27.60	27.60	2.11	5.67
2i	6.34	2.27	4.31	4.08	2.28	340.50	2.76	376.76	413.54	3.06	323.08	33.60	12.72	1.27	5.07
2j	6.36	2.28	4.32	4.08	2.28	357.05	2.99	397.87	439.05	3.53	337.10	26.96	16.77	2.92	8.62
2k	6.34	2.27	4.30	4.08	2.27	358.06	2.87	400.71	439.62	3.53	337.10	26.53	9.80	1.43	10.23
2l	6.35	2.27	4.31	4.07	2.28	358.19	3.24	392.34	433.26	3.58	357.05	19.56	17.66	5.99	7.92
2m	6.34	2.67	4.51	3.66	2.77	423.26	5.04	476.67	526.30	2.15	420.10	33.44	29.31	10.5	6.70
3a	6.36	2.84	4.60	3.52	3.01	338.38	1.43	334.00	361.86	3.49	295.05	23.78	30.26	23.94	1.07
3b	6.32	2.83	4.57	3.49	2.99	282.12	1.00	280.20	297.81	2.16	249.01	15.50	15.50	4.83	6.65
4	6.29	2.58	4.44	3.72	2.65	306.36	7.62	326.56	348.95	2.79	277.05	41.05	13.73	30.75	8.40
5a	6.98	2.87	4.92	4.10	2.96	303.60	6.20	332.41	357.86	3.88	297.04	55.87	40.75	56.7	19.34
5b	6.52	2.85	4.69	3.67	3.00	255.22	6.20	276.04	292.66	2.55	251.00	39.71	14.69	35.34	11.05
6a	6.24	2.42	4.33	3.81	2.46	425.36	11.41	444.11	486.86	5.41	368.14	20.54	13.51	14.15	3.39
6b	5.79	2.36	4.07	3.43	2.42	465.10	9.75	479.77	525.56	5.04	398.15	7.33	5.94	21.92	5.73
6c	6.57	2.44	4.50	4.13	2.46	424.93	11.02	465.21	508.89	4.41	397.13	34.53	47.37	20.15	3.58
6d	6.55	2.50	4.53	4.05	2.53	309.73	9.71	342.18	368.04	3.36	294.09	3.79	3.72	25.95	7.12

on the cytotoxic activity against the tested cells (Table 3). The statistical parameters R^2, R^2_{adj}, and SD were determined by considering compounds **1a–2a** and **2c–6d** (Table 4) and the subdivision of the tilted compounds into subclasses with the same base skeleton, **2a**, **2c–2m** (Table 5), **2a**, **2c–2f** (Table 6), and **2g–2m** (Table 7). By considering compounds **1a–2a** and **2c–6d** (Table 4), the SLR statistical parameters revealed that the influence of each separate descriptor on the observed cytotoxicity was relatively weak and varied with the

Table 4: Correlation coefficients (R^2), adjusted correlation coefficients (R^2_{adj}), and SDs of SLR between chosen descriptor and cell lines considering compounds **1a–2a** and **2c–6d**

Descriptors/SLR on cells	A459			HepG2			MCF-7			WRL68		
	%R^2	%R^2_{adj}	SD	%R^2	%R^2_{adj}	SD	%R^2	%R^2_{adj}	SD	%R^2	%R^2_{adj}	SD
IP	37.57	34.59	10.50	31.05	27.76	12.12	31.64	34.74	11.81	16.64	12.67	3.58
EA	6.33	1.87	12.86	2.63	−2.00	14.4	36.83	33.83	11.62	0.26	−4.99	3.92
χ	23.48	19.83	11.62	15.84	11.83	13.39	48.90	46.47	10.45	6.15	1.68	3.80
η	7.06	2.63	12.81	9.66	5.36	13.87	1.57	−3.11	14.51	8.90	4.56	3.75
S	7.38	2.97	12.79	9.40	5.09	13.89	1.63	−3.05	14.51	9.61	5.30	3.73
ω	4.92	0.4	12.96	1.98	−2.69	14.45	32.90	29.70	11.98	0.02	−4.74	3.92
α	3.10	−1.52	13.08	1.38	−3.31	14.45	0.00	−4.76	14.63	12.56	8.40	3.69
DM	2.26	−2.39	13.14	3.05	−1.57	14.37	13.24	9.11	13.62	2.28	−2.37	3.88
A	0.97	−3.75	13.23	4.43	−0.12	14.27	0.10	−4.66	14.62	7.14	2.72	3.78
V	0.95	−3.77	13.23	4.37	−0.18	14.27	0.16	−4.59	14.61	7.10	2.67	3.78
log P	4.82	0.28	12.97	0.81	−3.91	14.53	4.91	0.39	14.62	9.07	4.74	3.74
M	0.24	−4.51	13.27	6.07	1.59	14.15	0.05	−4.71	14.62	5.55	1.05	3.81

Table 5: Correlation coefficients (R^2), adjusted correlation coefficients (R^2_{adj}), and SDs of SLR between chosen descriptor and cell lines considering compounds **2a** and **2c–2m**

Descriptors/SLR on cells	A459			HepG2			MCF-7			WRL68		
	$\%R^2$	$\%R^2_{adj}$	SD	$\%R^2$	$\%R^2_{adj}$	SD	$\%R^2$	$\%R^2_{adj}$	SD	$\%R^2$	$\%R^2_{adj}$	SD
IP	58.92	54.82	5.42	31.96	25.15	10.66	64.21	60.64	8.24	4.22	−5.35	2.63
EA	36.11	29.73	6.77	23.61	15.97	11.30	51.52	46.67	9.60	3.68	−5.95	2.63
χ	51.77	46.95	5.88	31.41	24.55	10.70	66.41	63.05	7.99	4.60	−4.94	2.62
η	5.67	−3.77	8.22	5.38	−4.09	12.57	13.44	4.78	12.82	1.08	−8.81	2.67
S	7.40	−1.86	8.15	6.62	−2.71	12.49	15.91	7.50	12.64	1.72	−8.11	2.66
ω	34.24	27.67	6.86	22.25	14.48	11.40	50.13	45.15	9.73	3.84	−5.77	2.63
α	31.24	24.36	7.02	32.53	25.78	10.62	34.36	27.80	11.16	0.04	−9.96	2.68
DM	32.94	26.23	6.93	26.44	19.08	11.08	55.85	51.43	9.16	3.63	−6.01	2.64
A	30.65	23.72	7.05	41.20	35.32	9.91	36.42	30.06	10.99	0.36	−9.60	2.68
V	30.08	23.09	7.08	39.48	33.42	10.05	35.55	29.11	11.06	0.36	−6.60	2.68
log P	10.74	1.81	8.00	2.87	−6.48	12.74	19.06	10.97	12.40	6.23	−3.15	2.60
M	30.50	23.55	7.06	36.95	30.64	10.26	37.51	31.27	10.89	0.20	−9.78	2.68

Table 6: Correlation coefficients (R^2), adjusted correlation coefficients (R^2_{adj}), and SDs of SLR between chosen descriptor and cell lines considering compounds **2a** and **2c–2f**

Descriptors/SLR on cells	A459			HepG2			MCF-7			WRL68		
	$\%R^2$	$\%R^2_{adj}$	SD	$\%R^2$	$\%R^2_{adj}$	SD	$\%R^2$	$\%R^2_{adj}$	SD	$\%R^2$	$\%R^2_{adj}$	SD
IP	94.22	92.22	1.98	61.63	48.84	2.57	73.38	64.51	6.66	6.02	−25.31	3.68
EA	32.04	9.39	7.00	12.01	−17.33	3.89	70.44	60.59	7.02	2.43	−30.09	3.74
χ	60.19	46.92	5.20	30.20	6.93	3.46	85.12	80.15	4.98	4.20	−27.73	3.71
η	0.10	−33.20	8.24	1.44	−31.41	4.12	22.33	−3.56	11.38	0.06	−33.25	3.79
S	0.50	−32.66	8.22	1.26	−31.65	4.12	25.29	0.39	11.16	0.40	−32.81	3.78
ω	29.54	6.05	6.92	8.90	−21.47	3.96	67.10	56.14	7.41	2.76	−29.65	3.74
α	1.19	−31.75	8.19	11.62	−17.84	3.90	16.60	−11.20	11.79	8.98	−21.36	3.62
DM	36.16	14.87	6.59	26.19	1.58	3.56	82.29	76.39	5.43	3.69	−28.42	3.72
A	0.19	−33.08	8.24	5.59	−25.88	4.03	4.92	−26.77	12.59	16.09	−11.88	3.47
V	0.19	−33.08	8.24	5.26	−26.32	4.04	5.13	−26.50	12.58	15.93	−12.09	3.48
log P	8.60	−21.86	7.88	6.34	−24.75	4.01	67.78	57.04	7.33	32.88	10.51	3.10
M	2.05	−30.61	8.16	11.75	−17.67	3.90	15.26	−12.98	11.88	13.39	−15.47	3.53

tested cells. For A549, HepG2, and WRL 68 cells, best correlations were observed with IP, with correlation coefficients of 37.57, 31.05, and 16.64%, respectively. For MCF-7 cells, the best correlation was obtained with IP with a correlation coefficient of 48.9%. The weak to moderate influence of individual descriptor on the cytotoxicity is in accordance with our previous studies reported on the cytotoxicity of the synthesized 2-thiophen-naphtho (benzo)oxazinone derivatives and *C. zedoaria* metabolites [22,29]. Ishihara et al. tested the influence of a set of molecular descriptors of tropolone-related compounds on the cytotoxicity against HSC-2, HSC-3, and HSG cells, and they found poor to moderate correlations (0–50%) between the CC_{50} of cells and the chosen 11 descriptors [15]. These correlations improved for the series of **2a** and **2c–2m** (Table 5), demonstrating correlation coefficients of 58.92, 41.20, and 66.41% for A549, HepG2, and MCF-7 cells, respectively. However, for WRL 68 cells, correlations were relatively weak. For the series of compounds **2a** and **2c–2f** (Table 6), the correlations between each descriptor and tested cells strongly improved. For instance, for A549 and MCF-7 cells, maximum correlations were obtained with IP and electronegativity, with correlation coefficients of 94.22 and 85.12%, respectively. For the last series, **2g–2m** (Table 7), the correlations were relatively weak. Based on this analysis, it can be concluded that, for the synthesized compounds, the strength of each descriptor in the observed cytotoxic activity against tested cells strongly depends on their basic skeletons. Thus, for

Table 7: Correlation coefficients (R^2), adjusted correlation coefficients (R^2_{adj}), and SDs of SLR between chosen descriptor and cell lines considering compounds **2g–2m**

Descriptors/SLR on cells	A459			HepG2			MCF-7			WRL68		
	$\%R^2$	$\%R^2_{adj}$	SD	$\%R^2$	$\%R^2_{adj}$	SD	$\%R^2$	$\%R^2_{adj}$	SD	$\%R^2$	$\%R^2_{adj}$	SD
IP	16.79	0.15	6.42	1.93	−17.69	8.56	19.63	3.56	3.49	10.66	−7.21	2.26
EA	28.51	14.22	5.95	40.60	28.37	6.66	48.51	38.21	2.79	6.76	−11.89	2.31
X	31.28	17.53	5.84	41.61	29.94	6.60	44.51	33.41	2.90	7.86	−10.56	2.30
H	25.66	10.79	6.07	39.28	27.14	6.73	52.26	42.71	2.69	5.69	−13.17	2.32
S	25.48	10.58	6.08	39.54	27.45	6.72	52.52	43.02	2.68	5.67	−13.20	2.32
Ω	27.93	135.51	5.98	40.75	28.89	6.65	49.35	39.22	2.77	6.58	−12.10	2.31
a	31.72	18.07	5.82	9.27	−8.87	8.23	9.18	−8.98	3.71	3.70	−15.56	2.35
DM	13.32	−4.01	6.56	39.83	27.80	6.70	65.61	58.73	2.28	2.60	−16.88	2.36
A	33.50	20.20	5.74	13.57	−3.72	8.03	13.55	−3.73	3.62	3.26	−16.09	2.35
V	32.26	17.72	5.79	11.81	−5.83	8.11	12.59	−4.90	3.64	3.05	−16.34	2.36
log P	0.98	−18.82	7.00	13.62	−3.66	8.03	24.03	8.83	3.39	0.35	−19.58	2.39
M	24.62	9.55	6.11	14.31	−2.82	8.00	18.89	2.67	3.51	3.91	−15.31	2.35

these subclasses, one may conclude that the cytotoxicity relatively depends on their ability of these compounds to provide and accept electrons (best correlations are obtained with IP and electronegativity).

For each cancer cell line, the impact of each descriptor on the cytotoxic activity of the tested derivatives was mainly reliant on the nature of the descriptor itself. For A459 cells, the descriptors AE, χ, ω, α, μ, V, log P, and M demonstrated no significant influence ($R^2 \approx 0$–3%), while modest correlations were obtained with η and S ($R^2 \approx 25\%$). In the case of HepG2 cells, the best correlation was recorded for IP, with an R^2 of 27%, and an SD of 0.34; the lowest correlation was observed with surface area (A), with an R^2 of 0.22% and an SD of 0.5. The η and S demonstrated similar effects to those observed with the A459 cell line. However, for MCF-7 cells, the best correlations were obtained with the hardness η and S descriptors, with an R^2 of 61 and 62%, respectively. In contrast to HepG2 cells, the IP descriptor demonstrated negligible influence on the cytotoxic activity of the tested derivatives against MCF-7 cells, with an R^2 and an SD of 61% and 0.54, respectively. Thus, SLR demonstrated that the cytotoxicity moderately correlated with M of the tested derivatives, with an R^2 of 22%. However, for A459 and HepG2 cells, SLR displayed extremely weak effects for M, with R^2 less than 2%.

3.2.2 MLR analysis

As shown in the SLR analysis, the influence of each descriptor on the cytotoxicity of the synthesized compounds against the tested cells strongly depended on the basic skeleton of these compounds. In an attempt to improve the correlations between the cytotoxicity of each of these series and their descriptors, MLR analysis was performed for each series considering all tested cell lines.

3.2.2.1 Considering all compounds

Equations (1)–(4) show the reliable descriptors dependent on the observed cytotoxic activities against the tested cell lines for all compounds (Table 8). The correlations are relatively moderate for A459, HepG2, and MCF-7 cells, with correlation coefficients of 41, 64, and 58%, respectively. However, for WRL 68 cells, the correlation was relatively weak, with a correlation coefficient of 26%. For A459, HepG2, and WRL 68 cells, IP demonstrated the strongest contribution in equations (1), (2) and (4) with regression coefficients of 35.42, 44.69, and 6.37, respectively. This may indicate that these compounds provide an electron to the targeted enzyme of the tested cells. In addition to the strongest contribution of IP in these models (1–2 and 4), some other descriptors show moderate contribution hydrophobicity. For instance, hydrophobicity (log P) has a negative contribution in models 1 and 4 with regression coefficients of 2.37 and 0.009, while it has a positive contribution for model 2 (a regression coefficient of 1.69). However, for MCF-7 cells, the electronegativity reported the strongest contribution with a regression coefficient of 44.27, which may indicate that the compounds accept electrons from the targeted enzyme in MCF-7 cells (equation (3)). The moderate and weak correlations may be attributed to the basic skeleton of the synthesized compounds. Table 8 displays the predicted

Table 8: Predicted percentage inhibition and residuals obtained by using MLR equations (1)–(4) and considering all compounds

CPs	A459 (equation (1))		HepG2 (equation (2))		MCF-7 (equation (3))		WRL68 (equation (4))	
	$(\ln P)_{Pred.}$	Resid.	$(\ln P)_{Pred.}$	Resid.	$(\ln P)_{Pred.}$	Resid.	$(\ln P)_{Pred.}$	Resid.
1a	32.09	10.55	27.31	18.69	13.90	12.85	8.80	2.35
1b	34.51	15.21	20.93	15.07	13.67	10.77	10.09	0.39
2a	38.27	0.92	38.30	1.7	16.58	9.40	9.62	5.12
2c	37.20	3.41	34.69	3.31	40.73	2.72	8.18	1.92
2d	21.91	2.12	29.21	5.79	5.18	11.74	5.82	0.05
2e	31.00	3.27	36.10	0.1	9.27	3.34	7.77	5.17
2f	38.05	3.08	52.50	8.5	26.82	8.89	8.07	0.04
2g	31.16	14.66	20.19	10.19	11.02	3.43	9.07	1.71
2h	30.85	3.25	30.78	2.78	11.17	9.06	8.78	3.11
2i	28.48	5.12	17.61	4.61	10.30	9.03	7.61	2.54
2j	27.82	0.86	16.92	0.08	10.70	7.78	7.25	1.37
2k	27.29	0.76	25.54	15.54	9.96	8.53	7.14	3.09
2l	27.32	7.76	13.17	4.83	10.75	4.76	7.14	0.78
2m	30.47	2.97	27.30	1.7	20.66	10.16	7.43	0.73
3a	28.11	4.33	26.30	3.7	21.41	2.53	7.47	6.40
3b	29.76	14.26	23.84	7.84	20.81	15.98	8.54	1.89
4	27.34	13.71	14.02	0.02	24.20	6.55	7.76	0.64
5a	48.92	6.95	44.98	3.98	43.75	12.95	11.44	7.90
5b	35.90	3.81	16.54	1.54	34.37	0.97	9.80	1.25
6a	19.07	1.47	9.04	4.96	22.39	8.24	4.68	1.29
6b	4.00	3.33	5.63	4.63	7.53	14.39	1.70	4.03
6c	33.15	1.38	33.13	13.87	29.49	9.34	7.43	3.85
6d	35.19	31.4	17.96	13.96	31.33	5.39	9.03	1.91

cytotoxic activities and residuals of the observed values. The best reproduction of the observed cytotoxicity values for A459, HepG2, MCF-7, and WRL 68 cells was obtained for compounds **2k**, **4**, **5b**, and **2f**, with residual values of 0.76, 0.02, 0.97, and 0.04, respectively (Table 8).

$$(\ln P)_{\text{Pred.}} = -189 + 35.42\text{IP} - 2.37 \log P \quad R^2 = 41.34\%;\ R^2_{\text{Adj}} = 35.47\% \text{ and } \text{SD} = 10.43 \tag{1}$$

$$(\ln P)_{\text{Pred.}} = -371 + 44.69\text{IP} - 3.37\mu + 3.77A - 3.17V + 1.69 \log P \quad R^2 = 63.71\%;\ R^2_{\text{Adj}} = 53.03\% \text{ and } \text{SD} = 9.77 \tag{2}$$

$$(\ln P)_{\text{Pred.}} = -176.42 + 44.27\chi - 0.02\alpha + 1.52\mu \quad R^2 = 57.62\%;\ R^2_{\text{Adj}} = 50.93\% \text{ and } \text{SD} = 10.01 \tag{3}$$

$$(\ln P)_{\text{Pred.}} = -27.88 + 6.37\text{IP} - 0.64\alpha - 0.009 \log P \quad R^2 = 26.00\%;\ R^2_{\text{Adj}} = 14.31\% \text{ and } \text{SD} = 3.54 \tag{4}$$

3.2.2.2 Considering compounds 2a and 2c–2m

Equations (5)–(8) and Table 9 represent the best correlations between the observed cytotoxic activities of the subclass of compounds (**2a** and **2c–2m**) against the tested cell lines. The improved correlations were observed compared to the ones obtained considering all compounds (equations (5)–(8)). Indeed, for A459, HepG2, MCF-7, and WRL 68 cells, the obtained correlation coefficients were 77, 83, 98, and 79%. In accordance with correlations obtained considering all compounds, the observed activities against A459 and HepG2 cells were strongly dependent on IP with regression coefficients of 41.51 and 46.74, respectively (equations (5) and (6)). For MCF-7 cells (equation (7)), the observed activities were strongly related to the electronegativity and EA of the tested compounds with a positive contribution of the former (a regression coefficient of 78.60) and a negative contribution of the latter (a regression coefficient of 74.58). In this model (equation (7)), dipole moment and hydrophobicity show a moderate contribution with regression coefficients of 14.15 and 6.83, respectively. For WRL 68 cells (equation (8)), the observed activity depended on several descriptors with different contributions. The softness, electronegativity, electrophilicity, and hardness show strongest effects with regression coefficients of 13.544, 1.615, 1.214, and 473, respectively; while dipole moment and hydrophobicity display moderate contributions (equation (8)). Similarly, the SD and residuals were improved (equations (5)–(8) and Table 9). The improved correlations between the observed cytotoxic activities and the selected descriptors may be

Table 9: Predicted percentage inhibition and residuals obtained by using MLR equations (5)–(8) and considering compounds **2a** and **2c–2m**

CPs	A459 (equation (5))		HepG2 (equation (6))		MCF-7 (equation (7))		WRL68 (equation (8))	
	$(\ln P)_{Pred.}$	Resid.	$(\ln P)_{Pred.}$	Resid.	$(\ln P)_{Pred.}$	Resid.	$(\ln P)_{Pred.}$	Resid.
2a	37.67	1.52	36.53	3.23	25.11	0.87	4.79	0.30
2c	40.26	0.354	36.38	1.77	37.77	0.24	6.31	0.05
2d	26.30	2.273	30.45	4.16	15.50	1.42	6.82	0.95
2e	32.93	1.344	39.25	3.42	13.06	0.45	12.36	0.58
2f	44.65	3.516	46.59	2.83	35.80	0.09	8.41	0.30
2g	23.69	7.191	18.22	7.77	6.96	0.63	11.26	0.48
2h	25.37	2.229	19.48	8.12	3.84	1.73	4.78	0.89
2i	25.53	8.07	13.71	0.99	−2.86	4.13	7.90	2.83
2j	27.30	0.342	17.74	0.97	6.39	3.48	7.43	1.19
2k	27.23	0.698	18.27	8.47	3.97	2.54	8.50	1.73
2l	22.51	2.95	12.88	4.78	4.66	1.33	7.77	0.15
2m	29.99	3.454	26.91	2.40	10.83	0.33	6.34	0.36

attributed to the fact that this subclass of compounds has the same basic skeleton and that these compounds only differ in the substituted groups.

$$(\ln P)_{\text{Pred.}} = -254.55 + 41.51\text{IP} + 0.20A - 1.2\log P - 0.16M \quad (5)$$
$$R^2 = 77.01\%;\ R^2_{\text{Adj}} = 63.87\% \text{ and } \text{SD} = 4.85$$

$$(\ln P)_{\text{Pred.}} = -315.47 + 46.74\text{IP} - 0.63\alpha + 0.66A \quad (6)$$
$$R^2 = 83.28\%;\ R^2_{\text{Adj}} = 77.01\% \text{ and } \text{SD} = 5.91$$

$$(\ln P)_{\text{Pred.}} = -203.58 - 74.58\text{EA} + 78.60\chi - 0.97\alpha + 14.15\mu + 0.73V + 6.83\log P \quad (7)$$
$$R^2 = 97.69\%;\ R^2_{\text{Adj}} = 94.92\% \text{ and } \text{SD} = 2.96$$

$$(\ln P)_{\text{Pred.}} = 3775 - 1615.39\chi + 473.64\eta - 13544S + 1214\omega + 1.71\alpha + 29.66\mu - 0.59V - 20\log P - 0.62M \quad (8)$$
$$R^2 = 79.21\%;\ R^2_{\text{Adj}} = -14.35\% \text{ and } \text{SD} = 2.74$$

3.2.2.3 Considering subclasses 2a and 2c–2f

By considering the subclasses **2a** and **2c–2f** of compounds, the correlations between the cytotoxic activities and the reliable descriptor were highly improved (equations (9)–(12) and Table 10). For instance, the correlation coefficient and SD obtained with A459 cells were 99.86% and 0.53, respectively. In agreement with the above results, IP demonstrated the strongest positive effect on the observed activity of the tested compounds against A459 cells with a correlation coefficient of 3.79; while hardness and hydrophobicity display strongest negative effects with correlation coefficients of 5.99 and 4.15, respectively. Similar behaviors were observed with HepG2, MCF-7, and WRL 68 cells. For HepG2, IP has the strongest effect with a regression coefficient of 13.34. For MCF-7, the electronegativity displays the strongest contribution with a moderate effect on electrophilicity contribution (equation (11)). Hardness (with a negative contribution of 8.70) shows the strongest effect on the activity of the tested compounds against WRL68 (equation (12)).

Table 10: Predicted percentage inhibition and residuals obtained by using MLR equations (9)–(12) and considering compounds **2a** and **2c–2f**

CPs	A459 (equation (9))		HepG2 (equation (10))		MCF-7 (equation (11))		WRL68 (equation (12))	
	$(\ln P)_{Pred.}$	Resid.	$(\ln P)_{Pred.}$	Resid.	$(\ln P)_{Pred.}$	Resid.	$(\ln P)_{Pred.}$	Resid.
2a	39.38	0.19	38.30	1.46	25.48	0.50	4.44	0.06
2c	40.82	0.21	40.98	2.83	39.20	1.19	6.18	0.08
2d	23.99	0.04	34.41	0.20	13.16	3.76	5.95	0.08
2e	34.35	0.08	36.70	0.87	18.61	6.00	12.89	0.05
2f	40.69	0.44	41.73	2.04	32.78	2.93	8.22	0.11

$$(\ln P)_{\text{Pred.}} = -173 + 3.79\text{IP} - 5.99\eta - 4.15 \log P \quad R^2 = 99.86\%;\ R^2_{\text{Adj}} = 99.45\% \text{ and SD} = 0.53 \tag{9}$$

$$(\ln P)_{\text{Pred.}} = -56.61 + 13.34\text{IP} + 0.02A \quad R^2 = 70.78\%;\ R^2_{\text{Adj}} = 41.55\% \text{ and SD} = 2.75 \tag{10}$$

$$(\ln P)_{\text{Pred.}} = -199.47 + 56.71\chi - 11.68\omega \quad R^2 = 87.93\%;\ R^2_{\text{Adj}} = 75.87\% \text{ and SD} = 5.49 \tag{11}$$

$$(\ln P)_{\text{Pred.}} = 68.97 - 8.70\eta - 10.02\mu + 1.71 \log P \quad R^2 = 99.93\%;\ R^2_{\text{Adj}} = 99.71\% \text{ and SD} = 0.18 \tag{12}$$

3.2.2.4 Considering compounds 2g–2m

For the latest subclasses **2g–2m**, the correlations were strongly reliant on the tested cells (equations (13)–(16) and Table 11). Indeed, the correlations were relatively moderate for A459 and HepG2 cells, with a correlation coefficient of 54% and SD values of 6.14 and 6.56, respectively. However, for MCF-7 and WRL 68 cells, the correlations were relatively good, with coefficient correlations of 96 and 99%, respectively. In equation (13) (A459 cells), IP has the strongest effect with a regression coefficient of 98.27. For HepG2 cells (equation (14)), the electronegativity showed the strongest effect. However, for WRL68, the softness displayed the strongest contribution with a regression coefficient of 58,834, while hydrophobicity displayed a moderate contribution with a correlation coefficient of 234.

$$(\ln P)_{\text{Pred.}} = -632.4 + 98.27\text{IP} + 0.35\eta - 0.29M \quad R^2 = 54.31\%;\ R^2_{\text{Adj}} = 8.36\% \text{ and SD} = 6.14 \tag{13}$$

$$(\ln P)_{\text{Pred.}} = -457 + 117.14\chi - 0.08V \quad R^2 = 53.92\%;\ R^2_{\text{Adj}} = 30.89\% \text{ and SD} = 6.56 \tag{14}$$

$$(\ln P)_{\text{Pred.}} = 401.16 + 12.98\text{IP} - 100.96A - 0.51M \quad R^2 = 96.41\%;\ R^2_{\text{Adj}} = 92.83\% \text{ and SD} = 0.95 \tag{15}$$

$$(\ln P)_{\text{Pred.}} = 5{,}814 - 58{,}834S + 3.69A - 242.81 \log P + 2.22M \quad R^2 = 98.8\%;\ R^2_{\text{Adj}} = 96.39\% \text{ and SD} = 0.41 \tag{16}$$

4 Conclusions

Quantum chemical calculations and statistical analyses allow a better understanding of the structure–cytotoxicity relation between cytotoxicity with electronic, steric, and hydrophobic descriptors of the synthesized pyridotriazolopyrimidines. The obtained results demonstrated that the cytotoxicity depends on the cell line type and the combined molecular descriptors. SLR analysis revealed that the correlation of each descriptor on the observed cytotoxicity is relatively weak to moderate by considering a whole series of compounds (37–49%), and its improved by considering subclasses of compounds with similar basic skeleton (85–95%). For these subclasses of compounds, the best correlations were obtained with IP and electronegativity, with correlation coefficients of 94.22 and 85.12%, respectively. In accordance with SLR analysis, MLR analysis reveals that correlations related to different models are relatively weak to moderate by considering a whole series of compounds (26–58%), and these correlations are strongly improved by considering subclasses of compounds with similar basic skeletons (63–99%). MLR models reveal that the influence and impact of different descriptors vary with the tested cell lines and subclasses of compounds. For instance, for **2a** and **2c–2f** series, IP has the strongest effect against HepG2, while for MCF-7, the electronegativity displays the strongest effect.

Table 11: Predicted percentage inhibition and residuals obtained by using MLR equations (13)–(16) and considering compounds **2g–2m**

CPs	A459 (equation (13))		HepG2 (equation (14))		MCF-7 (equation (15))		WRL68 (equation (16))	
	$(\ln P)_{\text{Pred.}}$	Resid.	$(\ln P)_{\text{Pred.}}$	Resid.	$(\ln P)_{\text{Pred.}}$	Resid.	$(\ln P)_{\text{Pred.}}$	Resid.
2g	19.66	3.16	18.03	7.58	6.96	0.63	10.58	0.20
2h	23.89	3.71	18.69	8.91	3.12	1.01	6.03	0.36
2i	26.25	7.35	15.44	2.72	0.61	0.66	4.70	0.37
2j	30.70	3.74	14.64	2.13	2.29	0.63	8.77	0.15
2k	30.23	3.70	13.15	3.35	2.06	0.63	10.18	0.05
2l	21.75	2.19	14.27	3.39	6.28	0.29	8.02	0.10
2m	31.71	1.74	30.08	0.77	10.50	0.00	6.71	0.01

Acknowledgments: The authors extend their appreciation to the Deanship of Scientific Research at King Saud University for funding this work through the research group project no. RG-1435-068.

Author contributions: Conceptualization: RA and HAA; software and data curation: EHA; writing—original draft preparation: RA, EHA, and HAA; revise-review and editing: NSA, HA, and MM; and funding acquisition: RA. All the authors have read and agreed to the published version of the manuscript.

Conflict of interest: The authors declare no conflict of interest.

References

[1] El-Sherief HAM, Youssif BGM, Abbas Bukhari SN, Abdelazeem AH, Abdel-Aziz M. Synthesis, anticancer activity and molecular modeling studies of 1,2,4-triazole derivatives as EGFR inhibitors. Eur J Med Chem. 2018;156:774–89.

[2] Abdel-Rahman HM, Rezvan RN, Hassanzadeh F, Khodarahmi GA, Mirzaei M, Rostami M, et al. Synthesis, characterization, cytotoxic screening, and density functional theory studies of new derivatives of quinazolin-4(3*H*)-one Schiff bases. Res Pharma Sci. 2017;12:444–55.

[3] Flefel EM, El-Sayed WA, Mohamed AM, El-Sofany WI, Awad HM. Synthesis and anticancer activity of new 1-thia-4-azaspiro[4.5]decane, their derived thiazolopyrimidine and 1,3,4-thiadiazole thioglycosides. Molecules. 2017; 22:170.

[4] Al-Salahi R, Alswaidan I, Marzouk M. Cytotoxicity evaluation of a new set of 2-aminobenzo[*de*]iso-quinoline-1,3-diones. Int J Mol Sci. 2014;15:22483–91.

[5] Abuelizz HA, Marzouk M, Ghabbour H, Al-Salahi R. Synthesis and anticancer activity of new quinazoline derivatives. Saudi Pharm J. 2017;25:1047–54.

[6] Bereznak JF, Chan DM-T, Geffken D, Hanagan MA, Lepone GE, Pasteris RJ, et al. Preparation of fungicidal tricyclic 1,2,4-triazoles, 2008 WO 2008103357 A1 20080828.

[7] Hou W, Luo Z, Zhang G, Cao D, Li D, Ruan H, et al. Click chemistry-based synthesis and anticancer activity evaluation of novel C-14-1,2,3-triazole dehydroabietic acid hybrid. Eur J Med Chem. 2017;138:1042–52.

[8] Lagoja IM. Pyrimidine as constituent of natural biologically active compounds. Chem Biodiver. 2007;2:1–50.

[9] Shinkichi S, Nanao W, Toshiaki K, Takayuki S, Nobuyuki A, Sinji M, et al. "Pyridine and pyridine derivatives". Ullmann's Encyclopedia of Industrial Chemistry. Weinheim, Germany: Wiley-VCH Verlag GmbH & Co; 2000.

[10] Abuelizz HA, Iwana NANI, Ahmad R, Anouar E-H, Marzouk M, Al-Salahi R. Synthesis, biological activity and molecular docking of new tricyclic series as α-glucosidase inhibitors. BMC Chem. 2019;13:52.

[11] Abuelizz HA, Taie HAA, Marzouk M, Al-Salahi R. Synthesis and antioxidant activity of 2-methylthio-pyrido[3,2-e]-[1,2,4]triazolo[1,5-*a*]pyrimidines. Open Chem. 2019;17:823–30.

[12] Souza JR, De Almeida Santos J, Ferreira RH, Molfetta MMC, Camargo FA, Maria Honório AJ, et al. A quantum chemical and statistical study of flavonoid compounds (flavones) with anti-HIV activity. Eur J Med Chem. 2003;38:929–38.

[13] Kikuchi O. Systematic QSAR procedures with quantum chemical descriptors. Quantitative StructureActivity Relationships-. 1987;6:179–84.

[14] Camargo A, Mercadante R, Honório K, Alves C, Da Silva A. A structure–activity relationship (SAR) study of synthetic neolignans and related compounds with biological activity against *Escherichia coli*. J. Mol. Struct.: THEOCHEM. 2002;583:105–16.

[15] Ishihara M, Wakabayashi H, Motohashi N, Sakagami H. Quantitative structure–cytotoxicity relationship of newly synthesized tropolones determined by a semiempirical molecular-orbital method (PM5). Anticancer Res. 2010;30:129–33.

[16] Stanchev S, Momekov G, Jensen F, Manolov I. Synthesis, computational study and cytotoxic activity of new 4-hydroxycoumarin derivatives. Eur J Med Chem. 2008;43:694–706.

[17] Yang H-l, Chen G-h, Li Y-q. A quantum chemical and statistical study of ganoderic acids with cytotoxicity against tumor cell. Eur J Med Chem. 2005;40:972–6.

[18] Carvalho M, Hawksworth G, Milhazes N, Borges F, Monks TJ, Fernandes E, et al. Role of metabolites in MDMA (ecstasy)-induced nephrotoxicity: an *in vitro* study using rat and human renal proximal tubular cells. Arch Toxicol. 2002;76:581–8.

[19] Mendes AP, Borges RS, Neto AMC, de Macedo LG, da Silva AB. The basic antioxidant structure for flavonoid derivatives. J Mol Model. 2012;18:4073–80.

[20] Sarkar A, Middya TR, Jana AD. A QSAR study of radical scavenging antioxidant activity of a series of flavonoids using DFT based quantum chemical descriptors – the importance of group frontier electron density. J Mol Model. 2012;18:2621–31.

[21] Anouar EH. A quantum chemical and statistical study of phenolic schiff bases with antioxidant activity against DPPH free radical. Antioxidants. 2014;3:309–22.

[22] Hamdi OAA, Anouar EH, Shilpi JA, Trabolsy ZBKA, Zain SBM, Zakaria NSS, et al. A quantum chemical and statistical study of cytotoxic activity of compounds isolated from *Curcuma zedoaria*. Int J Mol Sci. 2015;16:9450–68.

[23] Tomasi J, Mennucci B, Cammi R. Quantum mechanical continuum solvation models. Chem Rev. 2005;105:2999–3093.

[24] Parr RG, Yang W. Density-Functional Theory of Atoms and Molecules. New York, NY, USA: Oxford University Press; 1989, Vol. 16.

[25] Koopmans T. Über die Zuordnung von Wellenfunktionen und Eigenwerten zu den einzelnen Elektronen eines Atoms. Physica. 1934;1:104–13.

[26] Neshev N, Mineva T. The role of interelectronic interaction in transition metal oxide catalysts. Metalligand interactions. Dordrecht, The Netherlands: Springer; 1996. pp. 361–405.

[27] Grigorov M, Weber J, Chermette H, Tronchet JM. Numerical evaluation of the internal orbitally resolved chemical hardness

tensor in density functional theory. Int J Quantum Chem. 1997;61:551–62.
[28] Mineva T, Sicilia E, Russo N. Density-functional approach to hardness evaluation and its use in the study of the maximum hardness principle. J Am Chem Soc. 1998;120:9053–8.
[29] Alshammari MB, Geesi MH, El Hassane A, Al-Salahi R, Alharthi AI, Elnakady Y, et al. Quantum chemical calculations and statistical analysis: structural cytotoxicity relationships of some synthesized 2-thiophen-naphtho(benzo)oxazinone derivatives. Cell Biochem Biophys. 2018;76:377–89.
[30] De Luca G, Sicilia E, Russo N, Mineva T. On the hardness evaluation in solvent for neutral and charged systems. J Am Chem Soc. 2002;124:1494–9.
[31] Frisch MJ, Trucks GW, Schlegel HB, Scuseria GE, Robb MA, Cheeseman JR, et al. Gaussian 16, Revision B.01. Wallingford, CT: Gaussian, Inc.; 2016.